

Cyclic Caged Morpholinos: Conformationally Gated Probes of Embryonic Gene Function**

Sayumi Yamazoe, Ilya A. Shestopalov, Elayne Provost, Steven D. Leach, and James K. Chen*

Deciphering the molecular mechanisms that underlie embryogenesis requires an ability to alter gene function with spatial and temporal precision. Synthetic reagents can be valuable tools in this discovery process, especially in model organisms currently intractable to targeted genomic changes. In particular, morpholino-based antisense oligonucleotides (MOs) have been widely used to inhibit gene expression in metazoans that develop ex utero (Figure 1a),^[1–4] and caged versions of these reagents (cMOs) can enable conditional gene silencing, by using targeted illumination.^[5–9] Composed of morpholino-based nucleosides and a phosphorodiamidate backbone, these nuclease-resistant probes are typically injected into zygotes as 25-base oligomers, after which they hybridize to complementary RNAs and disrupt splicing or translation. While cMOs can provide important new insights into embryonic gene function, their utility has been hindered by their empirical design, synthetic complexity, in vivo instability, reliance on complementary inhibitors, and/or use of multiple caging groups. Herein, we describe next-generation cMOs that overcome these limitations. We demonstrate that cyclic cMOs are effective reverse-genetic tools in zebrafish embryos, and we use these reagents to examine the timing of exocrine fate commitment in the developing pancreas.

We previously developed hairpin cMOs that can be activated with either ultraviolet (UV; 360 nm) or two-photon irradiation (Figure 1b).^[5,10] The RNA-targeting MO is tethered to a shorter, complementary MO inhibitor through a dimethoxynitrobenzyl (DMNB)- or bromohydroxyquinoline (BHQ)-based linker, thereby forming a hairpin structure that is resistant to RNA hybridization. Photocleavage of the linker separates the two oligonucleotides, allowing the 25-base MO to interact with its RNA target. Hairpin cMOs have been used to conditionally inactivate the expression of several zebrafish genes, including *no tail-a* (*ntla*), *floating head* (*flh*),

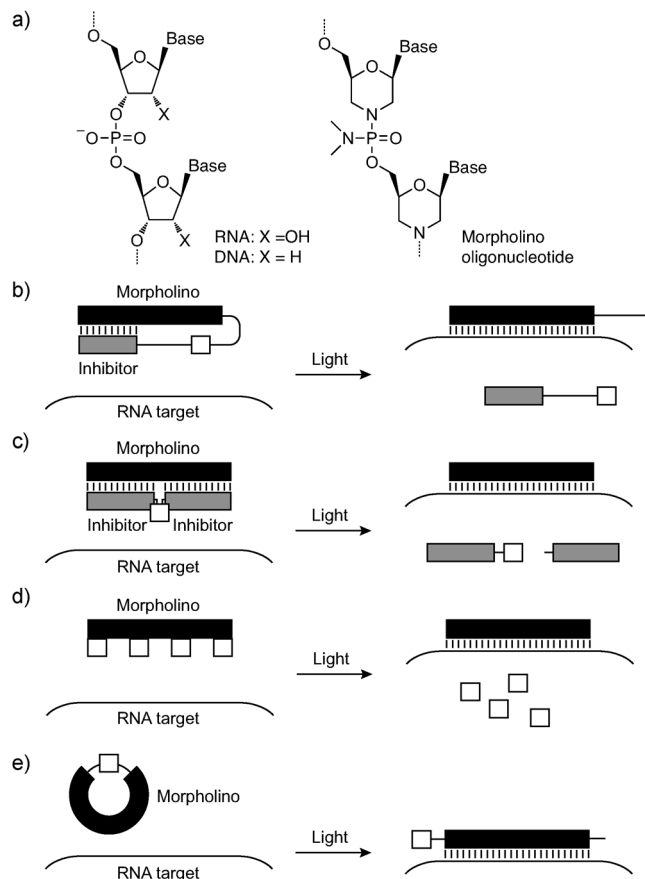


Figure 1. MOs and their caged derivatives. a) Comparison of DNA/RNA and MO chemical formulas. b) Hairpin caged MO. c) MO/caged oligonucleotide duplex. d) MO with caged bases. e) Cyclic caged MO. RNA-targeting MOs are shown in black, inhibitory oligonucleotides in gray, and caging groups in white.

heart of glass (*heg*), and *ETS1-related protein* (*etsrp*).^[5,10] We have also combined *ntla* cMOs, with caged fluorophores, fluorescence-activated cell sorting, and microarray technologies to dynamically profile the *Ntla*-dependent transcriptome.^[11] Despite these successes, hairpin cMOs have limitations. Their design involves careful optimization of the thermodynamics of inhibitor binding, their purification requires high-performance liquid chromatography (HPLC), and the inhibitory oligonucleotide can increase MO toxicity.

Other oligonucleotide caging strategies have been developed, each with its own advantages and disadvantages. For example, chimeras of peptide nucleic acid (PNA) and 2'-O-methyl (2'-OMe) RNA that form hairpins have been used to conditionally inhibit gene function,^[6] although the photo-released 2'-OMe RNAs may be toxic to embryos.^[7] Duplexes composed of the targeting MO and two complementary,

[*] Dr. S. Yamazoe, Dr. I. A. Shestopalov, Prof. Dr. J. K. Chen
Departments of Chemical and Systems Biology and Developmental
Biology, Stanford University School of Medicine
269 Campus Drive, CCSR 3155, Stanford, CA 94305 (USA)
E-mail: jameschen@stanford.edu
Homepage: <http://chen.stanford.edu>

Dr. E. Provost, Prof. Dr. S. D. Leach
Departments of Surgery, Oncology, and Cell Biology, McKusick-
Nathans Institute of Genetic Medicine, Johns Hopkins University
733 N. Broadway, BRB 471, Baltimore, MD 21205 (USA)

[**] We thank A. Puri and I. Hinkson for their assistance. This work was
supported by the NIH (R01 GM087292 and DP1 OD003792 to
J.K.C.; R01 DK061215 to S.D.L.).

Supporting information for this article (experimental details) is
available on the WWW under <http://dx.doi.org/10.1002/anie.201201690>.

tandem oligonucleotides connected by a nitrobenzyl-based linker have also been reported (Figure 1c).^[7,9] While these duplexes are easier to prepare than hairpin reagents, they release two potentially cytotoxic oligonucleotides upon photocleavage and can be less stable in vivo. Finally, MOs containing four nitropiperonyloxymethyl-caged thymine bases have been synthesized, bypassing the need for an inhibitory oligomer (Figure 1d).^[8] Activating these reagents, however, requires the photolysis of multiple caging groups per oligonucleotide, which can be difficult to achieve without damaging levels of UV irradiation.

To overcome these limitations, we sought to develop cMOs that are easier to synthesize, rely on a single caging group, and do not involve a complementary inhibitor. Because oligonucleotide duplexes have limited tolerance for bending,^[12] we hypothesized that cyclized MOs with a photocleavable linker could be used for conditional gene silencing (Figure 1e). A recent report that circular DNA oligonucleotides bind inefficiently to their complementary RNAs in vitro lends further support to this concept.^[13]

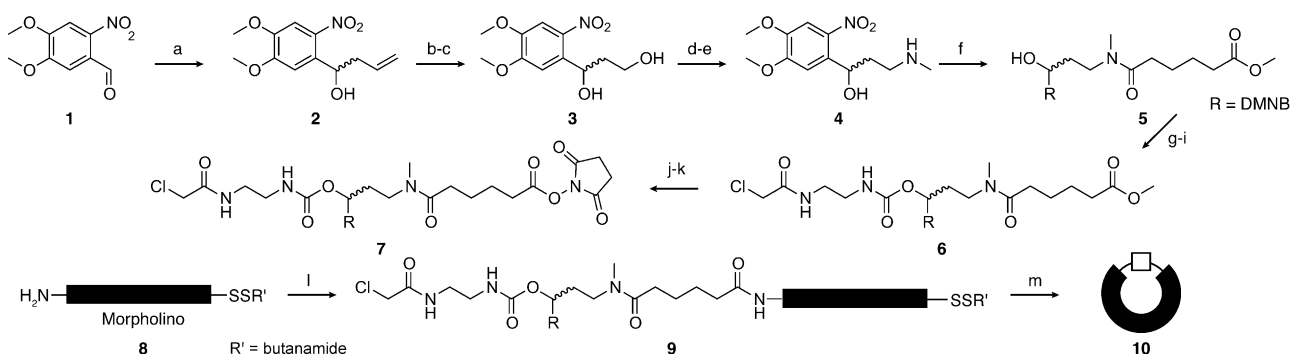
We tested this new caging strategy by targeting *ntla*, the zebrafish orthologue of mammalian *Brachyury*.^[14–16] Loss-of-function phenotypes for this T-box transcription factor include ablation of the notochord and posterior mesoderm, ectopic medial floor plate cells, and somite mispatterning. We synthesized a DMNB-functionalized linker with an *N*-hydroxysuccinimide ester and a chloroacetamide group **7** (Scheme 1) and reacted it with a 25-base *ntla* MO **8** (Supporting Information, Table S1) containing 5'-amine and 3'-alkyl disulfide modifications. Reduction of the linear MO-linker intermediate **9** yielded the free thiol, which spontaneously reacted with the chloroacetamide to give the desired macrocycle **10**. Liquid chromatography–mass spectrometry (LC–MS) analysis indicated that the macrocyclization reaction went to completion, and the final product was purified by gel filtration. The total yield for the 25-base cyclic *ntla* cMO synthesis starting with the linker and the targeting MO was 80 %, approximately a tenfold improvement over our hairpin cMO protocol.^[10]

We next investigated the efficacy of the cyclic *ntla* cMO in zebrafish embryos. Because we had previously shown that the

a linear *ntla* MO recreates the *ntla* mutant phenotype at a dose of 1 ng per embryo,^[5,10] we injected an equivalent amount of the photocleavable cyclic *ntla* cMO into zygotes and irradiated a subset of the embryos with UV light for ten seconds at 3 h post fertilization (hpf).^[15] The embryos were cultured until 24 hpf, at which point their phenotypes were scored according to four morphological classes (Figure 2a).^[10] The cyclic *ntla* cMO was found to be comparable to the hairpin cMO reagent in terms of efficacy, if not slightly better, with approximately 75 % ($n = 24$) of the cyclic cMO-injected embryos exhibiting no developmental defects in the absence of UV light and 90 % ($n = 20$) showing a complete *ntla* mutant phenotype following UV irradiation (Figure 2b). Western blot analysis of 10-hpf zebrafish confirmed the UV light-dependent loss of Ntla protein in cyclic *ntla* cMO-injected embryos (Figure 2c). The cyclic *ntla* cMO could also be used to knockdown *ntla* function in a spatially restricted manner; photoactivation of the reagent within the embryonic shield at 6 hpf converted notochord progenitors into medial floor plate cells, as has been reported with hairpin *ntla* cMOs (Figure 2d).^[5,11]

In principle, the basal activity of cyclic cMOs should decrease with macrocycle size, as bending within the smaller MO macrocycles will be more acute. To test this, we synthesized nonphotocleavable cyclic MOs corresponding to 21-, 23-, and 25-base oligonucleotides that target the *ntla* sequence (Table S1 and Scheme S1). The cyclic MOs or the corresponding linear MOs were then mixed with equimolar amounts of 25-base complementary RNA (Table S1), and melting curves were recorded (Table 1). Although these in vitro assays cannot recreate the complexity of MO/RNA interactions in vivo, the thermodynamic insights they provide can be informative.^[10] As expected, the cyclic MOs exhibited reduced affinities for RNA compared to the linear MOs, and greater differences in T_m and ΔG values were recorded as MO length decreased.

We next tested photoactivatable versions of these cyclic MOs and their linear counterparts in zebrafish embryos. As before, we UV-irradiated a subset of the cMO-injected embryos at 3 hpf and evaluated their morphological phenotypes at 24 hpf and Ntla protein levels at 10 hpf. Although the



Scheme 1. Cyclic *ntla* cMO synthesis. a) allyltrimethylsilane, TiCl_4 , CH_2Cl_2 , 98 %; b) O_3 , MeOH; c) NaBH_4 , MeOH, 74 % over 2 steps; d) tosyl chloride, pyridine, 63 %; e) methylamine, tetrahydrofuran (THF), 87 %; f) methyladipoyl chloride, *N,N*-diisopropylethylamine (DIPEA), CH_2Cl_2 , 57 %; g) 1,1'-carbonyldiimidazole, CH_2Cl_2 ; h) ethylenediamine, CH_2Cl_2 ; i) 2-chloroacetyl chloride, Et_3N , CH_2Cl_2 , 54 % over 3 steps; j) LiOH, THF, H_2O ; k) *N,N'*-disuccinimidyl carbonate, pyridine, CH_3CN , 68 % over 2 steps; l) 5'-amine, 3'-alkyl disulfide *ntla* MO (21-, 23-, or 25-base), 0.1 M $\text{Na}_2\text{B}_4\text{O}_7$, pH 8.5, dimethylsulfoxide (DMSO), 69–95 %; m) tris(2-carboxyethyl)phosphine (TCEP) resin, 0.1 M Tris-HCl buffer, pH 8.4, 84–92 %.

cyclic *ntla* cMOs exhibited less basal activity as they decreased in size, they also had an equivalent loss of efficacy upon photocleavage (Figure 2b–c). Linear versions of the 21-

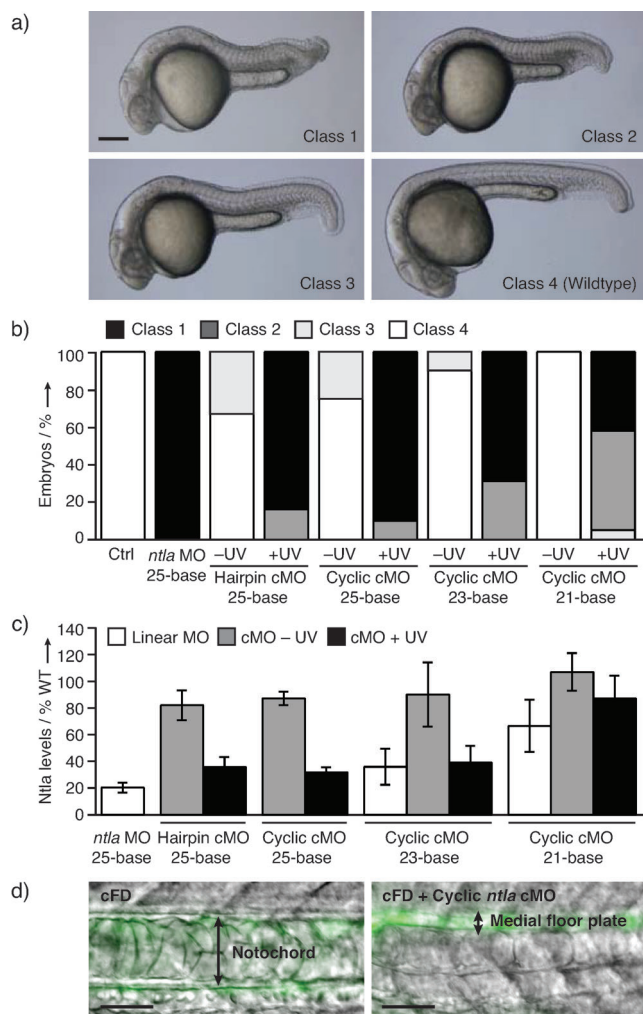


Figure 2. Comparison of cyclic and hairpin *ntla* cMOs. a) Classification of *ntla* loss-of-function phenotypes. 24-hpf embryos are shown, anterior to the left and dorsal at the top. Scale bar = 200 μ m. b) Phenotypic distributions for embryos injected with the indicated oligonucleotides and either cultured in the dark or irradiated with UV light at 3 hpf. Between 13 and 24 embryos were analyzed for each condition. c) Ntla protein levels in 10-hpf embryos subjected to the indicated conditions. Data are the average of at least four experiments (6 embryos per condition) \pm standard error of the mean (s.e.m.), normalized with respect to β -actin. d) Phenotypes observed in embryos injected with caged fluorescein-conjugated dextran (cFD) \pm the cyclic *ntla* cMO and irradiated within the shield at 6 hpf. Trunk regions of 36-hpf embryos are shown as overlays of differential interference contrast (DIC) and fluorescence micrographs (anterior left, dorsal up). Scale bars = 50 μ m.

Table 1: Thermodynamic parameters of MO/RNA duplexes.

| MO oligomer ^[a] | T_m [$^{\circ}$ C] linear ^[b] | ΔG [kcal mol ⁻¹] linear ^[b] | T_m [$^{\circ}$ C] cyclic ^[b] | ΔG [kcal mol ⁻¹] cyclic ^[b] | ΔT_m [$^{\circ}$ C] ^[c] | $\Delta\Delta G$ [kcal mol ⁻¹] ^[c] |
|----------------------------|---|--|---|--|---|---|
| 25-base | 78.3 \pm 0.9 | -22.1 \pm 2.3 | 75.2 \pm 1.2 | -18.5 \pm 0.7 | 3.1 \pm 0.7 | 3.6 \pm 0.9 |
| 23-base | 77.0 \pm 2.0 | -20.4 \pm 2.0 | 68.7 \pm 1.3 | -15.9 \pm 1.0 | 8.3 \pm 0.9 | 4.5 \pm 0.9 |
| 21-base | 74.2 \pm 1.3 | -19.7 \pm 1.1 | 60.2 \pm 1.3 | -14.0 \pm 0.4 | 14.0 \pm 1.1 | 5.7 \pm 0.7 |

[a] See Table S1 for sequence information. [b] Average values of 3–12 experiments \pm standard deviation (s.d.). [c] Absolute differences between linear MO/RNA and cyclic MO/RNA duplexes \pm standard error (s.e.).

and 23-base reagents were similarly less potent, indicating that this activity reduction is due to diminished MO/RNA interactions. Thus, for this method, the 25-base cyclic cMO provides the best dynamic range of caged and uncaged activities.

To test the generality of cyclic cMOs, we synthesized a 25-base cMO targeting *pancreas transcription factor 1 alpha* (*ptfla*; Table S1), which is required for exocrine cell differentiation in the developing pancreas.^[17–19] Ptf1a is selectively expressed in pancreatic exocrine cells, and their formation can therefore be directly visualized in transgenic zebrafish that express enhanced green fluorescent protein (eGFP) under the control of *ptfla* promoter-derived cis-regulatory elements (*Tg(ptfla:eGFP)* zebrafish).^[20] We injected *Tg(ptfla:eGFP)* zygotes with the cyclic *ptfla* cMO at a dose of 2 ng per embryo and UV irradiated a subset of the embryos at 3 hpf for ten seconds. Another set of *Tg(ptfla:eGFP)* zygotes was injected with an equivalent amount of a hairpin *ptfla* cMO that was designed according to previously established thermodynamic parameters.^[10] The intensity of eGFP fluorescence within the pancreatic field at three days post fertilization (dpf) was then scored for each experimental condition (Figure 3a).

The hairpin *ptfla* cMO partially impeded pancreatic development even without photoactivation, possibly because of linker degradation or the ability of the hairpin to interconvert between stem-loop and linear forms during the three-day period (Figure 3b). In contrast, the majority of *Tg(ptfla:eGFP)* zygotes injected with the cyclic *ptfla* cMO developed normally in the absence of UV light (76%, $n = 21$) but failed to form an exocrine pancreas upon UV irradiation (95%, $n = 21$; Figure 3b). Endocrine pancreas development was not affected, as gauged by whole-mount in situ hybridization with an antisense probe for *insulin* (Figure S1). These findings demonstrate the general efficacy of cyclic cMOs and suggest that they might be better probes of later embryological processes than hairpin-based cMOs.

To conclude these studies, we used the cyclic cMO technology to examine the temporal requirements of *ptfla* function for exocrine pancreas formation. We linearized the cyclic *ptfla* cMO in zebrafish with UV irradiation conditions optimized for various developmental stages (3–52 hpf; Figure S2). We then assessed exocrine tissue development at 3 dpf by whole-mount in situ hybridization with antisense *trypsin* (Figure 4) and *ptfla* (Figure S1) probes. The transcription levels of these exocrine markers followed similar trends, with a substantial decrease in transcript levels upon UV irradiation up to 44 hpf. Linearization of the *ptfla* cMO at 48 and 52 hpf, however, had only minor effects on their expression. Assuming that cyclic *ptfla* cMO efficacy is not lost during these studies (MOs can persist in zebrafish for up to

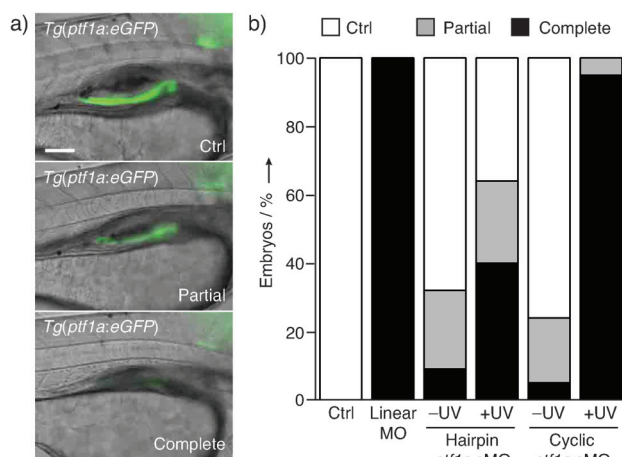


Figure 3. Comparison of cyclic and hairpin *ptf1a* cMOs. a) Classification of *ptf1a* loss-of-function phenotypes according to pancreas-specific eGFP expression in *Tg(ptf1a:eGFP)* zebrafish. Fluorescence micrographs of 3-dpf larvae are shown, anterior to the right and dorsal at the top. Scale bar = 100 μ m. Ctrl = control without oligonucleotide injected. b) Phenotypic distributions for embryos injected with the indicated reagents and either cultured in the dark or UV irradiated at 3 hpf. Between 21 and 31 embryos were analyzed for each condition.

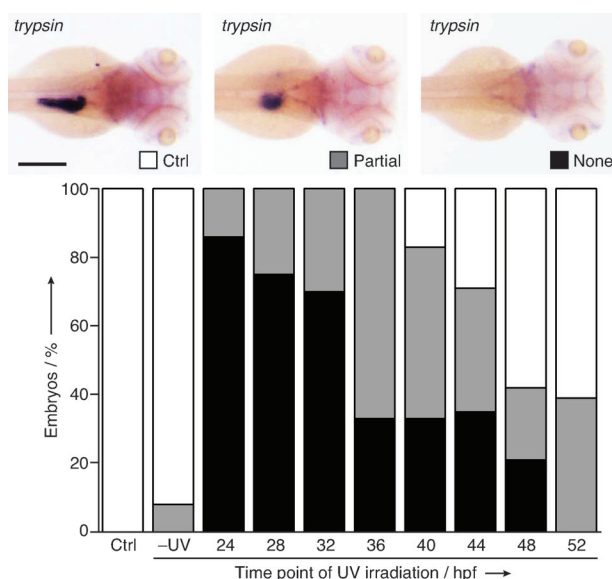


Figure 4. Temporal analysis of *ptf1a*-dependent exocrine pancreas development. Classification of *trypsin* expression levels and phenotypic distributions observed for embryos injected with the cyclic *ptf1a* cMO and either cultured in the dark or UV irradiated at the designated time points. Dorsal views of 3-dpf larvae are shown, anterior to the right. Scale bar = 200 μ m.

five days^[21]), our results suggest that pancreatic cells may be committed to exocrine cell fates as early as 2 dpf.

Taken together, our findings demonstrate the efficacy of cyclic cMOs as reverse-genetic tools for embryological studies and highlight their potential advantages over hairpin-based reagents. Cyclic cMOs can be synthesized in two steps starting

from commercially available oligonucleotides and linker **7**, and they can be purified without HPLC. They also bypass the need for inhibitory oligomers and multiple caging groups. Our results further suggest that these cyclic cMOs might be better than current cMO technologies for studying organogenesis and other late-stage developmental processes. These attributes should facilitate the implementation of cMOs by the developmental biology community and enhance future efforts to decipher embryonic gene function.

Received: March 1, 2012

Revised: April 24, 2012

Published online: June 11, 2012

Keywords: antisense oligonucleotides · developmental biology · gene expression · oligonucleotides · zebrafish

- [1] J. Summerton, D. Weller, *Antisense Nucleic Acid Drug Dev.* **1997**, *7*, 187–195.
- [2] J. Heasman, M. Kofron, C. Wylie, *Dev. Biol.* **2000**, *222*, 124–134.
- [3] A. Nasevicius, S. C. Ekker, *Nat. Genet.* **2000**, *26*, 216–220.
- [4] J. S. Eisen, J. C. Smith, *Development* **2008**, *135*, 1735–1743.
- [5] I. A. Shestopalov, S. Sinha, J. K. Chen, *Nat. Chem. Biol.* **2007**, *3*, 650–651.
- [6] X. Tang, S. Maegawa, E. S. Weinberg, I. J. Dmochowski, *J. Am. Chem. Soc.* **2007**, *129*, 11000–11001.
- [7] A. J. Tomasini, A. D. Schuler, J. A. Zebala, A. N. Mayer, *Genesis* **2009**, *47*, 736–743.
- [8] A. Deiters, R. A. Garner, H. Lusic, J. M. Govan, M. Dush, N. M. Nascone-Yoder, J. A. Yoder, *J. Am. Chem. Soc.* **2010**, *132*, 15644–15650.
- [9] A. Tallafuss, D. Gibson, P. Morcos, Y. Li, S. Seredick, J. Eisen, P. Washbourne, *Development* **2012**, *139*, 1691–1699.
- [10] X. Ouyang, I. A. Shestopalov, S. Sinha, G. Zheng, C. L. Pitt, W. H. Li, A. J. Olson, J. K. Chen, *J. Am. Chem. Soc.* **2009**, *131*, 13255–13269.
- [11] I. A. Shestopalov, C. L. W. Pitt, J. K. Chen, *Nat. Chem. Biol.* **2012**, *8*, 270–276.
- [12] J. Ramstein, R. Lavery, *Proc. Natl. Acad. Sci. USA* **1988**, *85*, 7231–7235.
- [13] X. Tang, M. Su, L. Yu, C. Lv, J. Wang, Z. Li, *Nucleic Acids Res.* **2010**, *38*, 3848–3855.
- [14] M. E. Halpern, R. K. Ho, C. Walker, C. B. Kimmel, *Cell* **1993**, *75*, 99–111.
- [15] S. Schulte-Merker, R. K. Ho, B. G. Herrmann, C. Nusslein-Volhard, *Development* **1992**, *116*, 1021–1032.
- [16] S. Schulte-Merker, F. J. van Eeden, M. E. Halpern, C. B. Kimmel, C. Nusslein-Volhard, *Development* **1994**, *120*, 1009–1015.
- [17] Y. Kawaguchi, B. Cooper, M. Gannon, M. Ray, R. J. MacDonald, C. V. Wright, *Nat. Genet.* **2002**, *32*, 128–134.
- [18] E. Zecchin, A. Mavropoulos, N. Devos, A. Filippi, N. Tiso, D. Meyer, B. Peers, M. Bortolussi, F. Argenton, *Dev. Biol.* **2004**, *268*, 174–184.
- [19] J. W. Lin, A. V. Biankin, M. E. Horb, B. Ghosh, N. B. Prasad, N. S. Yee, M. A. Pack, S. D. Leach, *Dev. Biol.* **2004**, *270*, 474–486.
- [20] H. Pisharath, J. M. Rhee, M. A. Swanson, S. D. Leach, M. J. Parsons, *Mech. Dev.* **2007**, *124*, 218–229.
- [21] B. R. Bill, A. M. Petzold, K. J. Clark, L. A. Schimmenti, S. C. Ekker, *Zebrafish* **2009**, *6*, 69–77.